Turkish Journal of Chemistry

http://journals.tubitak.gov.tr/chem/

Research Article

Turk J Chem
(2015) 39: 207 – 216

doi:10.3906/kim-1406-30

Fluorescent mono- and tetra-dansylated cavitands: synthesis and acid sensitivity

Ümit İŞCİ*, Yunus ZORLU, Fabienne DUMOULIN
Department of Chemistry, Gebze Technical University, Gebze Kocaeli, Turkey

Received: 12.06.2014 • **Accepted/Published Online:** 22.08.2014 • **Printed:** 30.04.2015

Abstract: Two fluorescent tetra- and mono-dansylated resorcinarene cavitands were prepared and fully characterized. The X-ray structure of mono-dansylated resorcinarene cavitand was obtained. Their intrinsic absorption and fluorescence properties were studied. These properties were strongly sensitive to the presence of perchloric acid, as evidenced by the appearance of isobestic points upon protonation of the dansyl dimethylamino functions. The decreasing of the fluorescence emission intensity upon titration with perchloric acid was explained by the excited state interactions between the dansyl groups of the resorcinarene. Fluorescence quantum yields (Φ_F) of mono- and tetra-dansylated cavitands and the reference compound were determined using dansyl chloride as reference in acetonitrile.

Key words: Resorcinarene, cavitand, dansyl, fluorescence, acid sensor

1. Introduction

Resorcinarenes are aromatic octols that can be converted into their cavitand forms, which are more rigid molecular systems and more stable in extreme conditions. The functionalized derivatives of resorcinarenes are widely investigated in fluorescence sensors, which have attracted significant interest because of their essential sensitivity and selectivity.[1–6] The dimethylamino function of dansyl moieties makes them particularly sensitive to pH variations, and the detection of acids is another application of dansylated compounds since the dansyl group exhibits a strong absorption band and a strong fluorescence in the visible region. Dansylated calixarenes,[7–12] cyclodextrins,[13] and resorcinarenes[14,15] have been employed as fluorescent chemosensors for metal detection. So far, dansylated resorcinarene cavitands have never been used as fluorescent sensors. The present works represent new insights in this field, as the superior stability of the cavitand form of resorcinarene, thanks to its more rigid and stable structure,[16] is beneficial for sensor applications that require stable materials for repeated uses and stability towards the detected species. In order to enlarge the choice of resorcinarene cavitands and to compare these new molecules with known dansylated calixarenes and resorcinarenes, we decided to prepare mono- and tetra-dansylated resorcinarene cavitands. Herein, we report the preparation, characterization, and fluorescence properties of tetra- (**3**) and mono- (**5**) *o*-dansylated resorcinarene cavitands (Scheme), characterized by ESI-MS, NMR (^{1}H and ^{13}C), UV-Vis, and FT-IR spectroscopic techniques. The X-ray structure of mono-dansylated cavitand **5** is reported. Electronic absorption and fluorescence properties of these two cavitands were investigated in acetonitrile. Two parameters, the contribution of the cavitand moiety and the effect of the number of dansyl units on the acid sensitivity, of **3** and **5** were investigated by comparing their fluorescence behavior in the presence of various concentrations of perchloric acid to the behavior of the reference compound **6**.

*Correspondence: u.isci@gyte.edu.tr

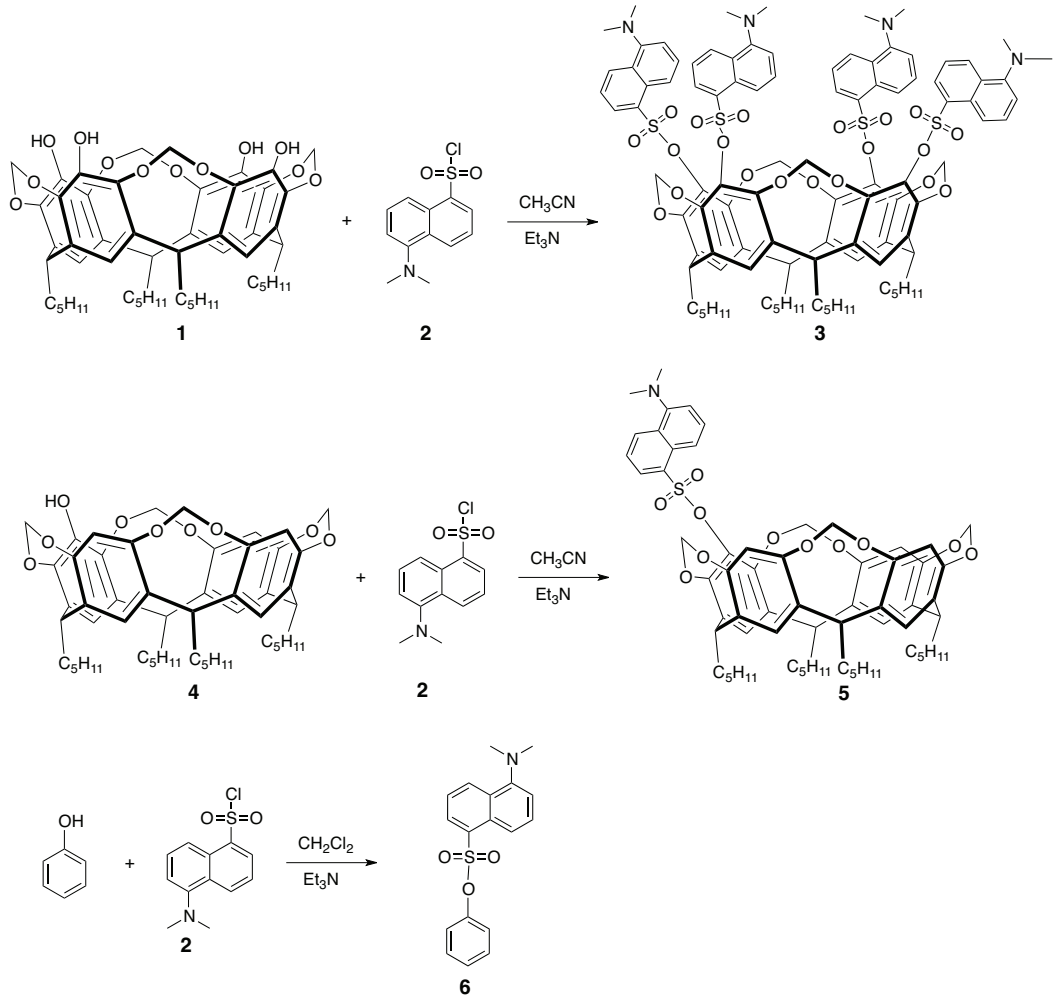

Scheme. Synthesis of tetra- and mono-dansylated cavitands **3** and **5** and of reference compound **6**.

2. Results and discussion

Tetra-dansylated cavitand **3** was prepared from tetra-hydroxylated resorcinarene cavitand **1**,[17] which reacted with dansyl chloride in acetonitrile in the presence of triethylamine in good yield (80%). Mono-dansylated cavitand **5** was prepared from mono-hydroxylated resorcinarene cavitand[18] **4** following the same protocol in 82% yield. Reference compound **6** was prepared according to a literature protocol[14] (Scheme).

The successful preparation of **3** and **5** was evidenced by mass spectroscopy. The ESI-MS spectrum of **3** exhibits a molecular peak at m/z = 1836.9 corresponding to a sodium adduct ($C_{100}H_{108}N_4O_{20}S_4Na$), and presenting an isotopic pattern identical to the simulated pattern with a maximum at m/z = 1836.6. The ESI-MS spectrum of **5** exhibits a unique molecular peak corresponding to the expected values of the molecular ion at m/z = 1066.6. The ^{1}H NMR spectrum of the resulting tetra-dansylated cavitand **3** displays one doublet indicative of an AB system (δA = 4.44 ppm, δB = 4.24 ppm) for the OCH_2O groups, and a singlet for the methyl groups of the dansyl unit at 2.9 ppm. Aromatic protons of tetra-dansylated cavitand **3** corresponding to the dansyl moieties are well distinguishable from the aromatic protons of the cavitand core: four doublets and two triplets for the aromatic protons of the dansyl groups, and a singlet for the aromatic protons of the

resorcinarene. The ^{1}H NMR spectrum of mono-dansylated cavitand **5** indicates a C_s symmetrical cavitand, showing the presence of two distinct AB patterns for the OCH_2O protons (at 5.73, 5.19, 4.54, and 4.35 ppm), and of two methine triplets (at 4.57 and 4.65 ppm).

Suitable crystals of cavitand **5** were grown by slow evaporation from acetonitrile at room temperature and its solid-state structure was established by single crystal X-ray structural analysis. Appropriate crystals of the tetra-dansylated derivative **3** could not be obtained despite attempts using different crystallization systems. The crystallographic analysis revealed that **5** crystallizes in the triclinic space group P-1 with two acetonitrile molecules in asymmetric units, as for a large number of crystal structures of resorcinarene.[19,20] As shown in Figures 1A and 1B, one of the acetonitrile molecules resides on the top of the cavitand bowl-shaped cavity, and the other one closely resides at the dansyl groups. The conformation is distorted, as the dihedral angles between pairs of opposite aromatic rings are 60.59° and 56.63°. The top rim diameters are 7.847 Å and 8.032 Å, and the lower rim diameters 5.253 Å and 5.250 Å.

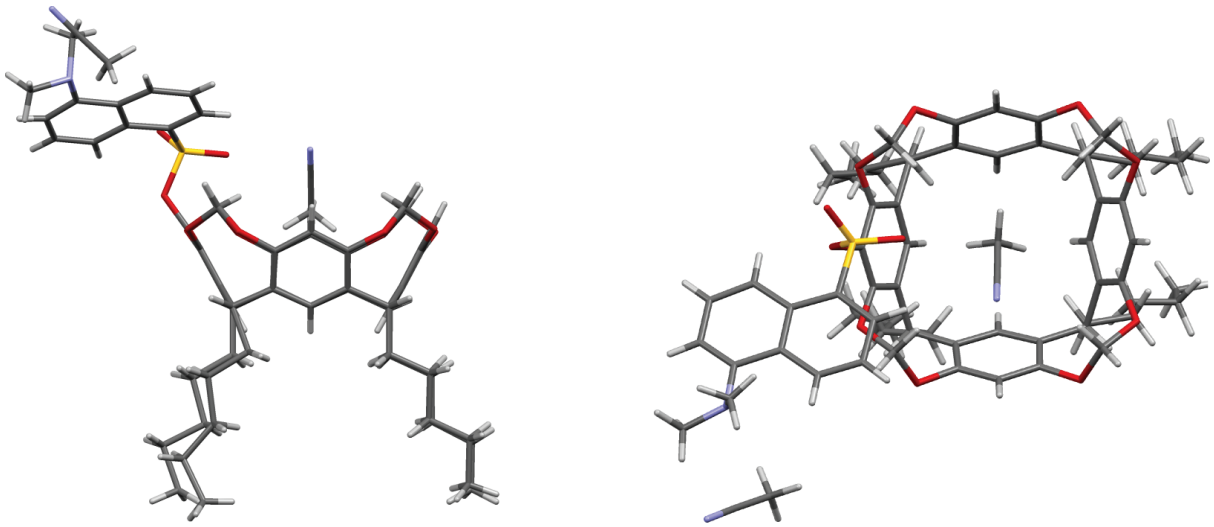

(a) (b)

Figure 1. (a) Side view and (b) top view of the crystal structure of **5**. $2(CH_3CN)$. One acetonitrile molecule is located inside the cavity and another acetonitrile molecule resides closely to the dansyl groups.

Table 1. Electronic absorption and fluorescence data for **3**, **5**, and **6**.

Compound	Absorption wavelength (nm)	log ε	Fluorescence emission wavelength (nm)	Quantum
3	354	4.44	541	0.79
5	342	4.29	521	0.75
6	350	4.12	555	0.72

Absorption and fluorescence spectra of tetra-dansylated cavitand **3**, mono-dansylated cavitand **5**, and reference compound **6** in acetonitrile are given in Figure 2. The absorption spectra of tetra-dansylated cavitand **3** and mono-dansylated cavitand **5** in different concentrations (from 2×10^{-6} to 10^{-5} mol L^{-1}) are given in Figure 3. Reference compound **6** exhibits absorption bands at 209, 275, and 360 nm. Both cavitands show maximal absorption bands in the near UV spectral region, at 351 nm for cavitand **3** and at 358 nm for cavitand **5** (Figures 2A and 2B). Absorption of cavitand **3** and cavitand **5** increased linearly together with the concentration (Figures 3A and 3B).

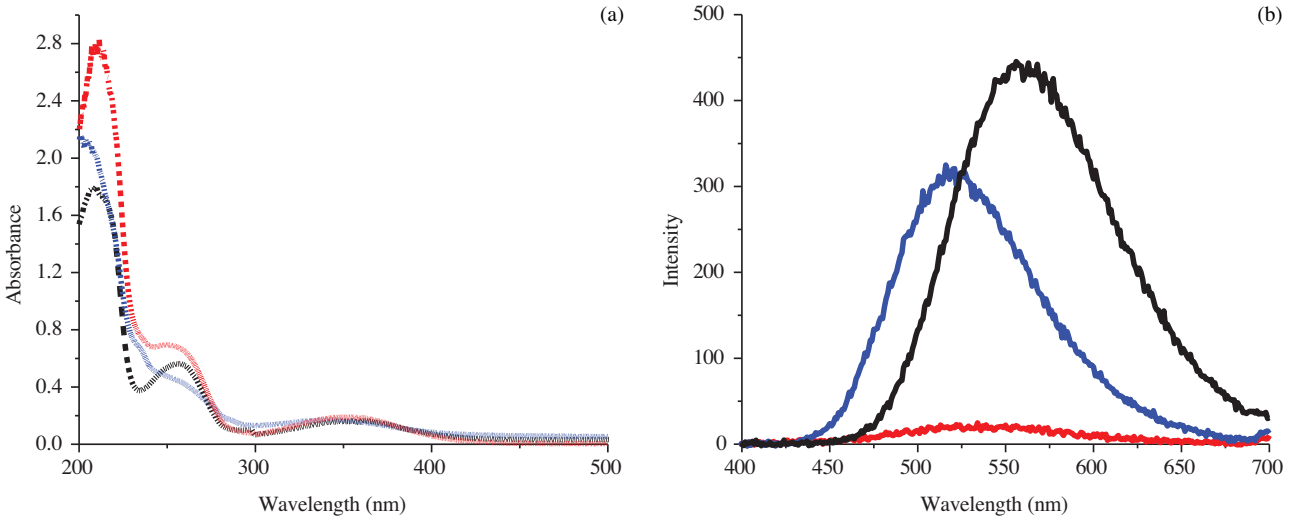

Figure 2. (A) Absorption and (B) emission spectra of cavitand **3** (red), cavitand **5** (blue), and reference **6** (black) in CH_3CN (λ_{exc} = 350 nm). Concentration: 1 × 10^{-5} mol L^{-1}.

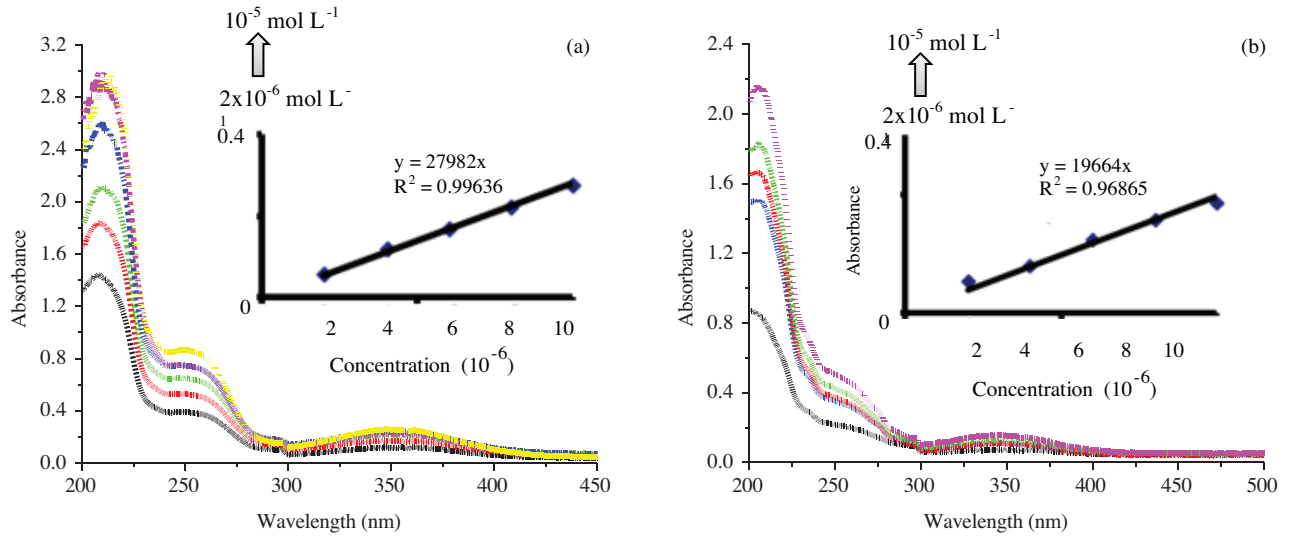

Figure 3. Absorption spectra of (A) cavitand **3** and (B) cavitand **5** in CH_3CN at different concentrations: 2 × 10^{-6} mol. L^{-1} (a), 4 × 10^{-6} mol. L^{-1} (b), 6 × 10^{-6} mol. L^{-1} (c), 8 × 10^{-6} mol. L^{-1} (d), 1 × 10^{-5} mol. L^{-1} (e). Inset: plot of absorbance at 350 nm versus concentration.

Reference compound **6** has the highest fluorescence intensity. While the number of dansyl groups in the cavitand increases, the fluorescence intensity decreases. The intensity of mono-dansylated cavitand **5** is higher than that of tetra-dansylated cavitand **3**. One can suggest that excited-state energy transfer between the dansyl groups of the cavitand is causing the reduction of emission, as has been observed in related dansylated resorcinarenes. It can be also explained that the excited-state energy transfer between the dansyls of the resorcinarene cavitand results in reduced emission.[14]

Table 2. Crystal data and refinement parameters for **5**.

Crystal parameters	**5**
Empirical formula	$C_{64}H_{75}NO_{11}S.2(C_2H_3N)$
Formula weight (g. mol^{-1})	1148.47
Temperature (K)	130(2)
Wavelength (Å)	0.71073
Crystal system	triclinic
Space group	*P*-1
a (Å)	10.542(1)
b (Å)	12.155(1)
c (Å)	24.071 (1)
α(°)	87.126(1)
β(°)	77.659(1)
γ(°)	84.653(1)
Crystal size (mm)	0.07 × 0.16 × 0.19
V (Å^3)	2998.6(4)
Z	2
ρ_{calcd} (Mg. cm^{-3})	1.272
μ (mm^{-1})	0.119
F(000)	1228
θ range for data collection (°)	0.866–25.026
h/*k*/*l*	–12/12, –14/14, 0/28
Measured reflections	49,274
Independent reflections (R_{int})	10,596 (0.052)
Absorption correction	Multiscan
T_{min} and T_{max}	0.88 and 0.99
Data/restraints/parameters	7816/192/820
Goodness-of-fit on F^2 (S)	0.93
$R[F^2 > 2s(F^2)]$	0.124
wR_2 (all data)	0.323
Largest diff. peak and hole (e.Å^{-3})	0.81 and –1.15

Fluorescence quantum yields (Φ_F) were determined by the comparative method (Eq. (1)), using dansyl chloride in acetonitrile (Φ_F = 0.07 in CH_3CN) as the reference:

$$\Phi F = \Phi F(Std)\frac{F.AStd.n^2}{FStd.A.n^2_{Std}} \quad (1)$$

where F and F_{Std} are the areas under the fluorescence emission curves of the samples and the standard, respectively. A and A_{Std} are the respective absorbances of the samples and standard at the excitation wavelengths. n^2 and n^2_{Std} are the refractive indices of solvent used for the sample and standard, respectively.

Electronic absorption and fluorescence data for cavitand **3**, **5**, and reference compound **6** are summarized in Table 1. Quantum yields of compound **3**, **5**, and **6** were obtained using emission spectra of dansyl chloride as standard. The quantum yield of cavitand **3** was 0.79 while it was 0.75 for cavitand **5**. The quantum yield of reference compound **6** was 0.72. These values are all in the same range. This is not contradictory with the lower fluorescence intensity observed for **3** relative to **5** and further works using femtosecond fluorescence spectroscopy will allow us to provide a detailed interpretation of the effect of the presence of several dansyl units, as performed on related calixarenes based dansylated derivatives.[7]

The dansyl group is known to be acid sensitive.[14] The fluorescence behavior of **3** and **5** upon addition of perchloric acid was investigated. The effect of acid concentrations on the absorption spectra of tetra-dansylated cavitand **3** and mono-dansylated cavitand **5** in acetonitrile is given in Figures 4A and 4B. Upon addition of perchloric acid, absorption spectra of cavitand **3** and cavitand **5** clearly change. The main absorption bands at 250 and 350 nm decrease and new absorption peaks appear at 286 and 220 nm. The protonation of the dimethylamino unit of the dansyl groups gives a new strong blue shifted absorption peak. The isosbestic points at 312, 273, and 234 nm confirm the protonation of dansyl groups.

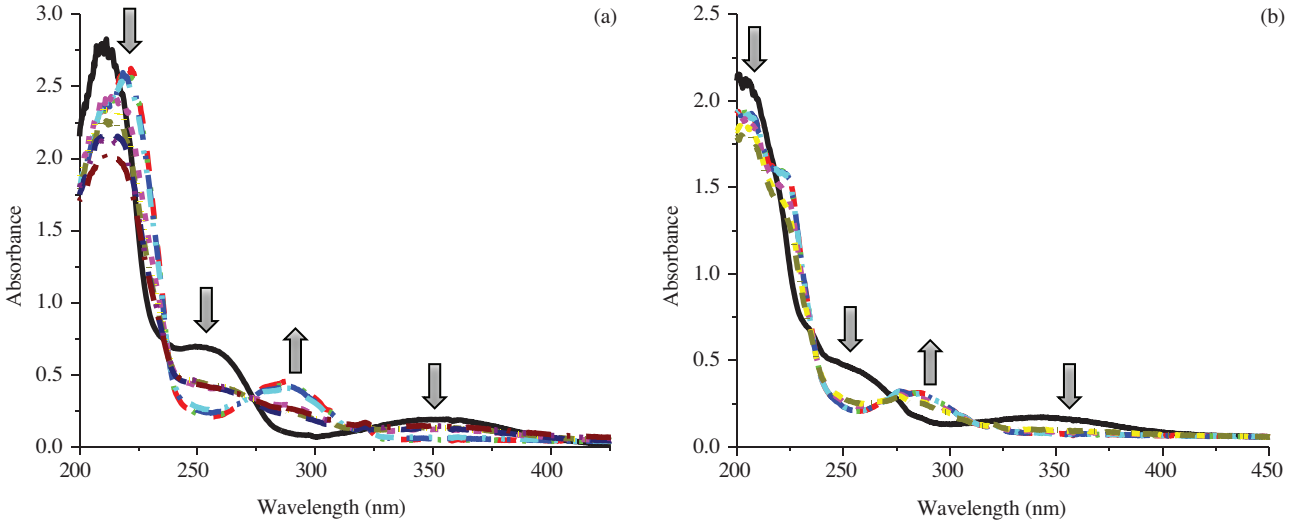

Figure 4. Absorption spectra of cavitand **3** (A) and **5** (B), c = 1 × 10^{-5} mol. L^{-1}, upon titration by perchloric acid (0.25, 0.5, 0.75, 1, 1.5, 2, 2.5, 3, and 4 equiv).

The emission spectra of cavitand **3** and cavitand **5** and their acidic forms after titration with perchloric acid are given in Figures 5A and 5B. The emission spectra show one band at 535 nm for tetra-dansylated cavitand **3** and one band at 521 nm for mono-dansylated cavitand **5**. The fluorescence intensities of cavitand **3** and **5** decrease while the concentration of perchloric acid increases. After addition of 0.5 equiv. perchloric acid, cavitand **3** does not exhibit a fluorescence band. Interestingly, the emission band at 550 nm for reference compound **6** shifts to 495 nm and fluorescence intensities decrease after addition of perchloric acid (Figure 5C). This is much more sensitive than the results obtained with tetra-dansylated octol resorcinarene[14] toward TFA, with tetra- and di-dansylated calixarenes using perchloric acid[7] in acetonitrile like we did. The enhanced fluorescence quenching of dansylated resorcinarenes is due to the efficient couplings of the excited states to the low-frequency vibrational modes of the resorcinarene structures, suggesting better hosting properties of resorcinarene in its cavitand form. The excited-state energy transfer between the dansyl groups of the resorcinarene cavitands results in decreasing emission intensity.[14]

Fluorescence quenching experiments of the dansylated cavitands and reference compound **6** were performed by the addition of different concentrations of perchloric acid to a fixed concentration of the mono and tetra-dansylated cavitands and reference **6**. The fluorescence spectra of all these dansylated compounds at each perchloric acid (PA) concentration were recorded and the changes in fluorescence intensity related to PA concentration by the Stern–Volmer (SV) equation (Eq. (2)):

$$\frac{I_0}{I} = 1 + K_{SV}[PA], \tag{2}$$

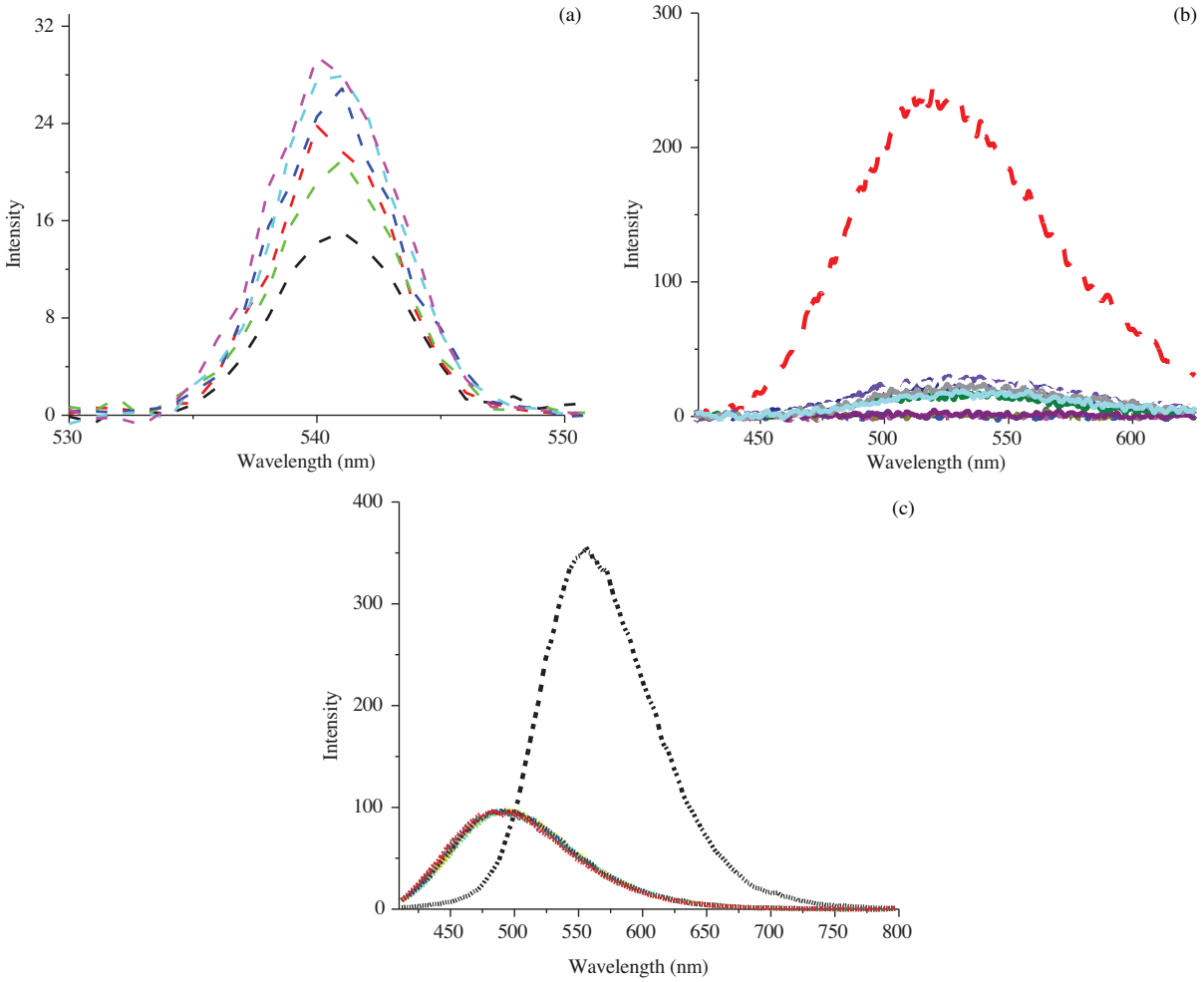

Figure 5. Fluorescence emission spectra of cavitand **3** (A) and **5** (B), and reference compound **6** (C) with perchloric acid titration. 1×10^{-5} mol. L^{-1}, (perchloric acid) = 0.25, 0.5, 0.75, 1, 1.5, 2, 2.5, 3, 4 equiv.

where I_0 and I are the fluorescence intensities of fluorophore in the absence and presence of quencher, respectively. K_{SV} is the Stern–Volmer constant.

Figures 6A and 6B show the quenching of cavitand **3** and cavitand **5** with perchloric acid in acetonitrile. Typical linear plots for perchloric acid with cavitand **3** were observed with an intercept at one evidencing that the dynamic character of the fluorescence quenching is dynamic, while this is not the case for the mono-dansylated derivative (cavitand **5**).

3. Conclusion

Tetra- and mono-dansylated resorcinarene cavitands **3** and **5** were prepared and fully characterized with ESI-MS, NMR (^{1}H, ^{13}C), IR, and UV-Vis spectroscopic techniques, and the X-ray structure of mono-dansylated cavitand **5** was obtained. The absorption and emission properties of cavitands **3** and **5** were studied upon titration with perchloric acid. Cavitands **3** and **5** were highly sensitive to perchloric acid. When perchloric acid was added, the absorption band decreased for both cavitands and new absorption bands were observed. The dimethylamino unit of the dansyl groups was easily protonated. A new strong blue shifted absorption peak confirms the protonated forms of the dansylated resorcinarene cavitands. The UV-Vis spectra of cavitand **3** and

5 exhibited isosbestic points evidencing the protonation of dimethylamino unit of dansyl groups. This shows the excited-state interactions of the dansylated **3** and **5**, resulting in decreasing emission. Quantum yields of compound **3**, **5**, and **6** were determined using emission spectra of dansyl chloride as standard.

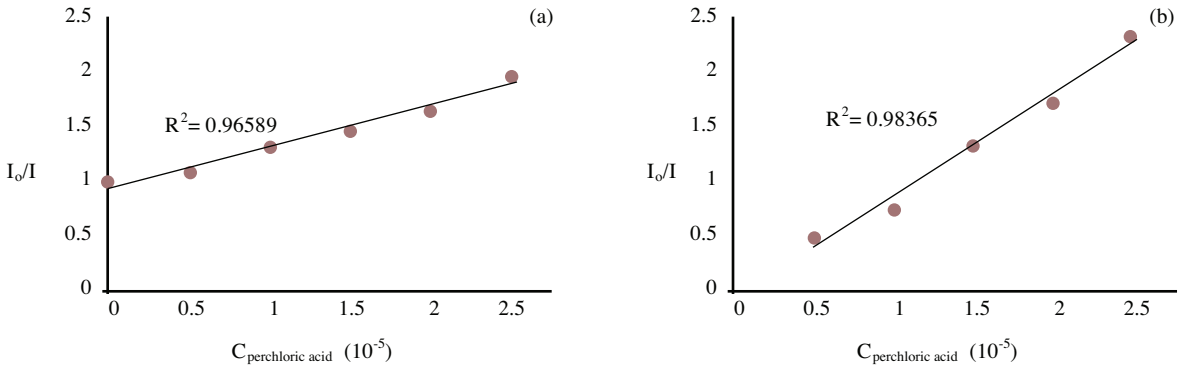

Figure 6. Stern–Volmer plots for PA quenching of cavitand **3** (A) and cavitand **5** (B).

4. Experimental section

4.1. Materials and methods

All solvents were dried before use as described by Perrin and Armarego in the literature.[21] Reagents were purchased from Sigma-Aldrich and used without further purification. Infrared spectra (IR) were recorded on a Bio-Rad FTS 175C FTIR spectrophotometer. UV visible absorption spectra were obtained using a Shimadzu 2001 UV spectrophotometer using a 1-cm path length cuvette at room temperature. Mass spectra were measured on a Bruker microTOF spectrometer equipped with an electronspray ionization (ESI) source. ^{1}H and ^{13}C NMR spectra were recorded in deuterated chloroform ($CDCl_3$) on a Varian 500 MHz spectrometer. Fluorescence emission spectra were recorded on a Varian Eclipse spectrofluorometer using 1-cm pathlength cuvettes at room temperature.

4.2. Synthesis

4.2.1. Preparation of tetra-dansylated resorcinarene cavitand 3

Tetra-OH cavitand **1** (0.25 g, 0.28 mmol) was dissolved in MeCN (20 mL) and Et_3N (0.17 mL, 1.25 mmol) was added in one portion with vigorous stirring. The reaction mixture was stirred for 15 min, and then dansyl chloride (0.337 g, 1.25 mmol) was added in one portion. The reaction mixture was stirred at room temperature for 24 h. The solvent was removed in vacuo. Pure tetra-dansylated resorcinarene cavitand was obtained by chromatography on SiO_2 (CH_2Cl_2) as a white powder. Yield: 0.415 g, 80%. ^{1}H NMR (500 MHz, $CDCl_3$): δ= 8.62 (d, 4H, *Dan*-H, J= 8.5 Hz), 8.25 (d, 4H, *Dan*-H, J= 8.7 Hz), 8.10 (d, 4H, *Dan*-H, J= 7.3 Hz), 7.57 (t, 4H, *Dan*-H, J = 7.9 Hz), 7.45 (t, 4H, *Dan*-H, J = 5.8 Hz), 7.24 (d, 4H, *Dan*-H, J = 7.6 Hz), 6.89 (s, 4H, arom. CH of resorcinarene), 5.44 and 4.24 (AB spin system, 8H, OCH_2O, J = 7.6 Hz), 4.85 (t, 4H, J = 7.6 Hz), 2.84 (s, 24H, $N(CH_3)_2$), 2.04–1.99 (m, 8H, $CHCH_2$), 1.28–1.17 (m, 24H, $CH_2CH_2CH_2CH_3$), 0.78 (t, 12H, CH_2CH_3, J= 7.1 Hz); ^{13}C NMR (125 MHz, $CDCl_3$): δ= 150.8, 146.7, 137.7, 134.5, 132.6, 130.5, 128.8, 128.7, 127.7, 127.6, 121.8, 118.5, 116.5, 114.5, 98.5, 44.4, 35.6, 30.8, 28.6, 26.3, 21.5, 13.1 ppm. ESI-MS: m/z 1836.9 $[M + Na]^+$; FT-IR (cm^{-1}) : 1177, 1364 (–SO_2).

4.2.2. Preparation of mono-dansylated resorcinarene cavitand 5

Mono-dansylated resorcinarene cavitand (**5**) was synthesized and purified as described above for **3**. The amounts of the reagents were: mono-OH cavitand **4** (0.125 g, 0.15 mmol), dansyl chloride (0.08 g, 0.30 mmol), Et_3N (0.04 mL, 0.30 mmol), and CH_3CN (10 mL). Yield: 0.131 g, 82%. ^{1}H NMR (500 MHz, $CDCl_3$): δ= 8.64 (d, 1H, *Dan*-H, J= 8.5 Hz), 8.33 (d, 1H, *Dan*-H, J= 8.5 Hz), 8.18 (d, 1H, *Dan*-H, J= 8.6 Hz), 7.59-7.53 (m, 2H, *Dan*-H), 7.22 (d, 1H, *Dan*-H, J = 7.6 Hz), 7.07 (d, 3H, arom. CH of resorcinarene, J = 7.9 Hz), 7.03 (s, 1H, arom. CH of resorcinarene), 6.52 (s, 1H, arom. CH of resorcinarene), 6.46 (s, 2H, arom. CH of resorcinarene), 5.73 (d, 2H, OCH_2O, J= 7.6 Hz), 5.19 (d, 2H, OCH_2O, J= 5.8 Hz), 4.72 (t, 2H, $CHCH_2$, J= 7.5 Hz), 4.65 (t, 2H, $CHCH_2$, J= 7.6 Hz), 4.54 (d, 2H, OCH_2O, J= 7.6 Hz), 4.35 (d, 2H, OCH_2O, J= 7.6 Hz), 2.92 (s, 6H, $N(CH_3)_2$), 2.21–2.12 (m, 8H, $CHCH_2$), 1.44–1.29 (m, 24H, $CH_2CH_2CH_2CH_3$), 0.91 (t, 12H, CH_2CH_3, J= 7.1 Hz); ^{13}C NMR (125 MHz, $CDCl_3$): δ= 154.0, 153.8, 153.6, 146.6, 138.4, 137.6, 137.2, 136.6, 134.2, 132.5, 130.6, 128.8, 127.7, 127.6, 121.9, 119.4, 119.3, 117.0, 115.7, 115.6, 114.5, 98.8, 98.3, 44.4, 39.8, 35.5, 35.3, 31.0, 30.9, 28.8, 28.7, 26.5, 26.4, 21.6, 13.0, 12.7 ppm. ESI-MS: m/z 1066.6 [M]$^+$; FT-IR (cm^{-1}): 1176, 1365 (–SO_2).

4.3. X-ray data collection and structure refinement

Single crystal X-ray diffraction analysis was carried out on a Bruker APEX II QUAZAR three-circle diffractometer with monochromatized Mo $K\alpha$X-radiation (λ = 0.71073 Å) using φ and ω technique at 130 (2) K. Indexing was performed using APEX2.[22] Data integration and reduction were carried out with SAINT V8.27B.[23] Absorption correction was performed by multiscan method implemented in SADABS V2012/1.[24] Space groups were determined using XPREP implemented in APEX2. The structure was solved using SIR-2004.[25] The least-square refinement on F^2 was achieved with the software CRYSTALS.[26] All nonhydrogen atoms were refined anisotropically. The hydrogen atoms were all located in a difference map, but those attached to carbon atoms were repositioned geometrically. The H atoms were initially refined with soft restraints on the bond lengths and angles to regularize their geometry (C—H in the range 0.93–0.98 Å) and U_{iso}(H) (in the range 1.2–1.5 times U_{eq} of the parent atom), after which the positions were refined with riding constraints. The crystals available for X-ray structural analysis were of quite poor quality and weak scatterers at high resolution (≈1.00 Å), thus resulting in comparatively high R values. C590, C600, C611, C621, C631 and C591, C601, C610, C620, C630 atoms in one of n-penthyl chains are disordered over two sites with occupancies of 0.7342:0.2658, whereas C441, C442, C443 and C45 C46, C47 atoms in the another n-penthyl chain are disordered over two sites with occupancies of 0.4285:0.5715. The crystallographic data and refinement details of the data collection for compound **5** are given in Table 2. The final geometrical calculations and the molecular drawings were carried out with the software PLATON[27] and MERCURY[28]. Crystallographic data for this structure have been deposited with the Cambridge Crystallographic Data Centre under CCDC 914896.

References

1. Inouye, M.; Hashimoto K.; Isagawa, K. *J. Am. Chem. Soc.* **1994**, *116*, 5517–5518.
2. Hayashi, Y.; Ichimura, K. *J. Photochem. Photobiol. A* **2002,** *149*, 199–206.
3. Sarmentero, M. A.; Ballester, P. *Org. Biomol. Chem.* **2007**, *5*, 3046–3054.
4. Sarmentero, M. A.; Ballester, P. *Org. Lett.* **2006**, *8*, 3477–3480.

5. de Silva, A. P.; Gunaratne, H. Q. N.; Gunnlaugsson, T.; Huxley, A. J. M.; McCoy, C. P.; Rademacher, J. T.; Rice, T. E. *Chem. Rev.* **1997**, *97*, 1515–1566.
6. Valeur, B. *Molecular Fluorescence. Principles and Applications*; Wiley-VCH: Weinheim, Germany, 2002, Chapter 10.
7. Metivier, R.; Leray I.; Valeur, B. *Photochem. Photobiol. Sci,* **2004**, *3*, 374–380.
8. Miao, R.; Zheng, Q.; Chen, C.; Huang, Z. *Tetrahedron Lett.* **2004**, *45*, 4959–4962.
9. Talanova, J. G.; Roper, E.; Buie, N.; Gorbunova, M.; Bartsch, R.; Talanov, V. *Chem. Commun.* **2005**, 5673–5675.
10. Gruber, T.; Fischer, C.; Felsmann, M.; Seichter, W.; Weber, E. *Org. Biomol. Chem.* **2009**, *7*, 4904–4917.
11. Ocak, Ü.; Ocak, M.; Bartsch, R. A. *Inorg. Chem. Acta.* **2012**, *381*, 44–57.
12. Pandey, S.; Azam, A.; Pandey, S.; Chawla, H. *Org. Biomol. Chem.* **2009**, *7*, 269–279.
13. Ikeda, H.; Nakamura, M.; Ise, N.; Oguma, N.; Nakamura, A.; Ikeda, T.; Toda, F.; Ueno, A. *J. Am. Chem. Soc.*, **1996**, *118*, 10980–10988.
14. Kodiah Beyeh, N.; Aumanen, J.; Ahman, A.; Luostarinen, M.; Mansikkamaki, H.; Nissinen, M.; Korppi-Tommola, J.; Rissanen, K. *New J. Chem.* **2007**, *31*, 370–376.
15. Bhatt, K. D.; Gupte, H. S.; Makwana, B. A.; Vyas, D. J.; Maity, D.; Jain, V. K. *J. Fluoresc.* **2012**, *22*, 1493–1500.
16. Gramage-Doria, R.; Armspach, D.; Matt, D. *Coord. Chem. Rev.* **2012**, *257*, 776–816.
17. Cram, D. J.; Jaeger, R.; Deshayes, K. *J. Am. Chem. Soc.* **1993**, *115*, 10111–10116.
18. Lützen, A.; Haß, O.; Bruhn, T. *Tetrahedron Lett.* **2002**, *43*, 1807–1811.
19. Aakeröy, C. B.; Schultheiss, N.; Desper, J. *CrystEngComm.* **2006**, *8*, 502–506.
20. Berghaus, C.; Feigel, M. *Eur. J. Org. Chem.* **2003**, 3200–3208.
21. Perrin, D.D.; Armarego, W. L. F. *Purification of Laboratory Chemicals*, 2nd Edn, Pergamon Press: Oxford, UK, 1989.
22. Bruker (2012) APEX2, version 2012.10-0, Bruker AXS Inc., Madison, Wisconsin, USA.
23. Bruker (2012) SAINT, version V8.27B, Bruker AXS Inc., Madison, Wisconsin, USA.
24. Bruker (2012) SADABS, version 2012/1, Bruker AXS Inc., Madison, Wisconsin, USA.
25. Burla, M. C.; Caliandro, R.; Camalli, M.; Carrozzini, B.; Cascarano, G. L.; De Caro, L.; Giacovazzo, C.; Polidori, G.; Spagna, R. *J. Appl. Cryst.* **2005**, *38*, 381–388.
26. Betteridge, P. W.; Carruthers, J. R.; Cooper, R. I.; Prout, K.; Watkin, D. J. *J. Appl. Cryst.* **2003**, *36*, 1487.
27. Spek, A. L. *Acta Cryst. D*, **2009**, *65*, 148–155.
28. Macrae, C. F.; Edgington, P. R.; McCabe, P.; Pidcock, E.; Shields, G. P.; Taylor, R.; Towler, M.; van de Streek, J. *J. Appl. Cryst.* **2006**, *39*, 453–457.